Electronic Supplementary Material (ESI) for

Hierarchical self-assembly of enantiopure and racemic helicenes at the liquid/solid interface: from 2D to 3D

Hai Cao,[a]§ Andrea Minoia,[b]§ Inge De Cat,[a] Johannes Seibel,[a]Deepali Waghray,[c] Zhi Li,[a] David Cornil,[b] Kunal S. Mali,[a] Roberto Lazzaroni,[b] Wim Dehaen,[c] and Steven De Feyter[a]*

[a]Department of Chemistry, Division of Molecular Imaging and Photonics, KU Leuven−University of Leuven, Celestijnenlaan 200-F, 3001 Leuven, Belgium

[b]Laboratory for Chemistry of Novel Materials Université de Mons-UMONS Place du Parc 20, B-7000 Mons (Belgium)

[c]Department of Chemistry, Division of Molecular Design and Synthesis, KU Leuven−University of Leuven, Celestijnenlaan 200-F, 3001 Leuven, Belgium

Contents:

Fig. S13. Close-up STM images and corresponding simulated models of surface-bound (*P*)-1 monomer, dimer and trimer

Fig. S14. High-resolution STM images and tentative structural models of the homochiral and racemic linear networks of helicenes

Fig. S15. Supplementary results of the self-assembled networks of (*P*)-1: (*M*)-1 = 95:5 at the TCB/Au(111) interface and simulated structure model for a *P-M* dimer

Fig. S16. STM images of the self-assembled networks of the mixtures of (*P*)-1and (*M*)-1 at the TCB/Au(111) interface.

Fig. S17. Additional large scale AFM images of the structures of (P)-1upon drop casting its TCB solution on Au(111)

Fig. S18. Additional large scale AFM images of the structures of (*rac*)-1upon drop casting its TCB solution on Au(111).

Experimental details

1.1 Synthesis of the target compounds (rac)-1 and (P)-1: (*rac*)-1 was synthesised according to previously reported literature procedure (Dehaen et al. *Org. Lett.*, **2011**, *13*, 5516-5519). Enantiopure form (*P*)-1 was obtained by separation of (*rac*)-1 on a chiral HPLC using ChiralPak IA column at room temperature using 0.7 mL/min flow rate. The column dimensions for a typical semi-prep chiral column are 20 × 250 mm. The mobile phase was heptane-ethanol 60/40 v/v under isocratic conditions. The enantiopurity was estimated by several preps to be > 98%.

1.2 Solution preparation: 1, 2, 4-trichlorobenzene (TCB, 99%, Sigma-Aldrich, used as received) and 1-phenyloctane (98%, Sigma-Aldrich, used as received) were used as solvent to dissolve (*P*)-1 and (*rac*)-1. The concentrations used in each experiment are specified in corresponding caption.

1.3 SEM measurements: Silicon wafers were dipped into acetone and cleaned with ultrasonic cleaner for 5-10 minutes. After that the silicon wafers were further washed with Milli-Q water and dried with argon flow. One droplet of helicene solution (~7 μL) were drop-casted on a slice of clean silicon wafer and then dried at ambient conditions. After the evaporation of solvent, the samples were coated with gold and characterized by SEM. At least two samples were prepared for each solution to reduce the uncertainty. SEM measurements were performed using a FEI-Quanta-250-FEG system with an accelerating voltage of 5 kV, 10 kV or 20 kV.

1.4 AFM measurements: AFM measurements were performed on graphite and Au(111) surface with size of around 1 cm × 1 cm. Prior to AFM imaging, two droplets of helicene solution (~15 μL) were casted on substrate and then dried at ambient conditions. AFM measurements were performed in air with a Multimode AFM with a Nanoscope IV controller (Veeco/Digital Instruments) in tapping mode.

1.5 STM measurements: All STM experiments were performed at room temperature (20–23°C) using a PicoSPM (Molecular imaging, now Agilent) machine operating in constant–current mode with the tip immersed in the supernatant liquid. STM tips were prepared by mechanical cutting from Pt/Ir wire (80%/20%, diameter 0.2 mm). Prior to imaging, a drop of the solution was applied onto a freshly cleaved surface of highly oriented pyrolytic graphite (HOPG, grade ZYB, Advanced Ceramics Inc., Cleveland, USA) or Au(111) films on mica (Georg Albert PVD Company). Typical parameters for the imaging of helicenes on both the graphite and gold surfaces are V_{bias} = -700-1100 mV and (I_{set}), and I_{set} = 50-150 pA, where V_{bias} and I_{set} are sample bias and tunneling current, respectively. For analysis purposes, recording of a monolayer image on HOPG was followed by consecutive imaging the graphite substrate underneath. This was done under the same experimental conditions but by lowering the substrate bias (typically V_{bias} = -1 mV) and increasing the tunnelling current (typical I_{set} = 800-900 pA). From the atomically-resolved STM image of HOPG, one can easily obtain the graphite symmetry axes. The images were corrected for drift via the Scanning Probe Image Processor (SPIP) software (Image Metrology ApS), using the graphite lattice, allowing a more accurate unit cell determination. From the corrected graphite images, three main symmetry axes and also three reference axes (normal to main symmetry axes) can be determined. The images are low-pass filtered.

1.6 Molecular modelling for (rac)-1 network on graphite: As a preliminary step in the modeling protocol, the force fields available in the Biovia's molecular modeling package Materials Studio were tested. The Dreiding force field, combined with atomic charges obtained from the Gasteiger method, was found to perform good description of the geometry of the helicene core. As initial guess for the structure of the modelled assembly, a periodic supercell is created by replicating 5 times the original periodic box along the unit cell vectors **a** and **b**. Next, the periodicity is removed from the monolayer so that it can be placed onto a larger, rigid, periodic graphene slab, to allow for a refinement of the monolayer structure. Such refinement is obtained by applying an MD/Quench iterative scheme, consisting in alternating structure optimization steps and molecular dynamic simulations. The structure optimization step is used to optimize a number of structures extracted from the previous MD trajectory and the lowest energy structure found is used as starting point for the new MD simulation. The scheme is iterated until there are no more meaningful variations in the parameters of the average unit cell for the monolayer. Since the modeling is conducted without explicit solvent, and to keep complexity at a manageable level, two of the four alkoxy groups that are attached to the helicene cores are first neglected, namely those attached to the part of the helix that is not in contact with the graphite. 50 ps-long MD simulations runs are conducted in the NVT ensemble at 250 K and to avoid breaking the non-periodic molecular assembly, the sulfur atoms are fixed in their initial position. The goal is to refine the orientation of the alkoxy groups. The subsequent structure optimizations (Quench step) are performed removing the constraints on the sulfur atoms.

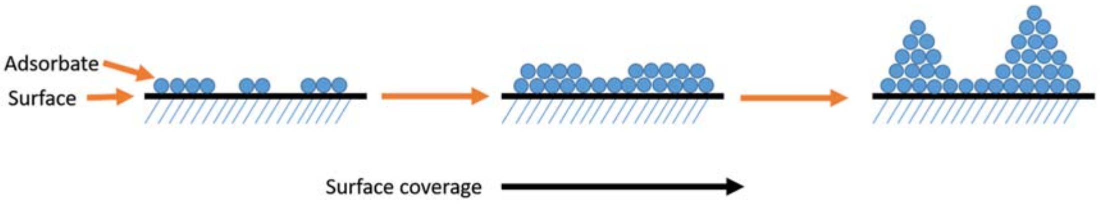

Scheme S1. Schematic illustration of the Stranski–Krastanov growth. For reference, see *Journal of Applied Physics.*, 2012, **111**, 044321.

Supplementary results

Table S1. Adsorption energy (kcal/mol) of coronene and hexadecane on different substrates.

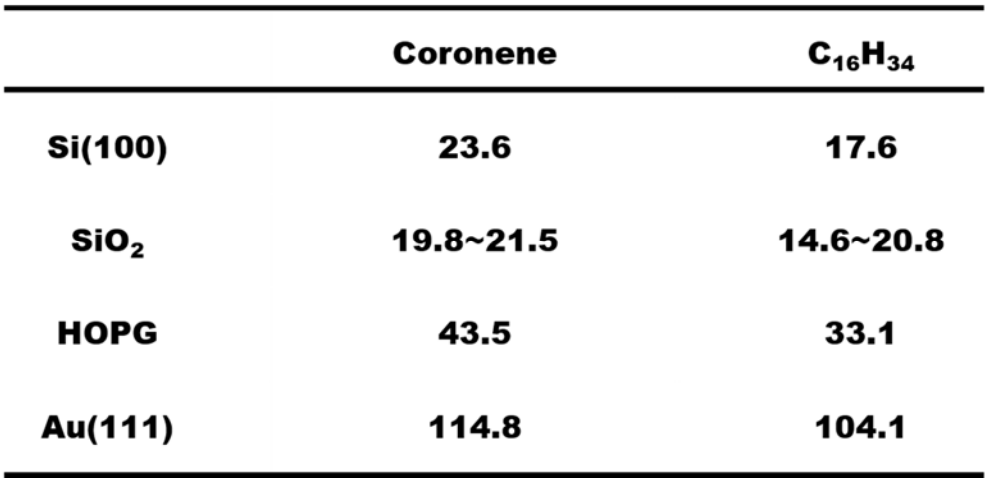

	Coronene	$C_{16}H_{34}$
Si(100)	23.6	17.6
SiO_2	19.8~21.5	14.6~20.8
HOPG	43.5	33.1
Au(111)	114.8	104.1

Method: Performed with Materials Studio, using the Forcite module with COMPASS force field. All simulations were performed under periodic boundary conditions. The substrates were frozen during the simulations, and a cutoff of 1.85 nm was applied for the van der Waals interactions. Initially, coronene or hexadecane was placed on top of periodic surfaces, along one of the symmetry axes of substrate. Different orientations were checked to reach optimum adsorption. Quartz crystal of SiO_2 was used to evaluate the impact of a oxidized layer on the adsorption of molecules on silicon, and the adsorption on different facets were simulated to check if there is a significant variation. The adsorption energies were calculated using $E_{adsorp} = E_A+E_S-E_{A-S}$, where E_A, E_S and E_{A-S} represent the calculated energies of the adsorbate, the substrate and the adsorbate on surface, respectively. Corresponding simulation results are displayed in the following Fig.:

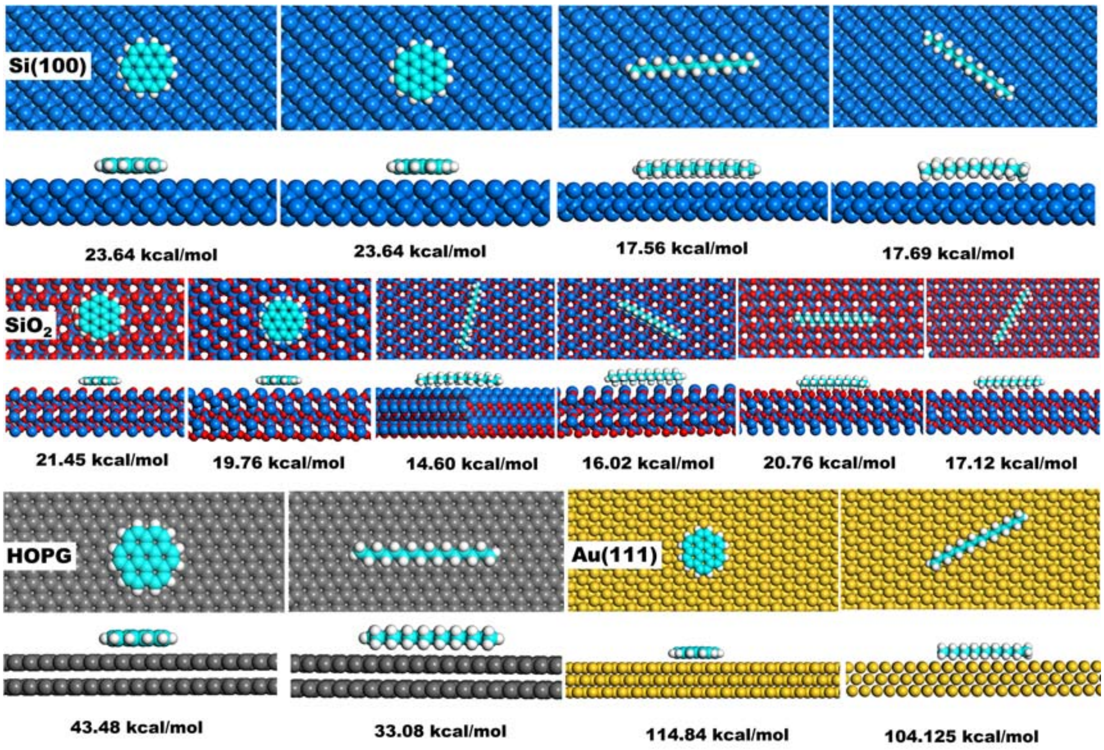

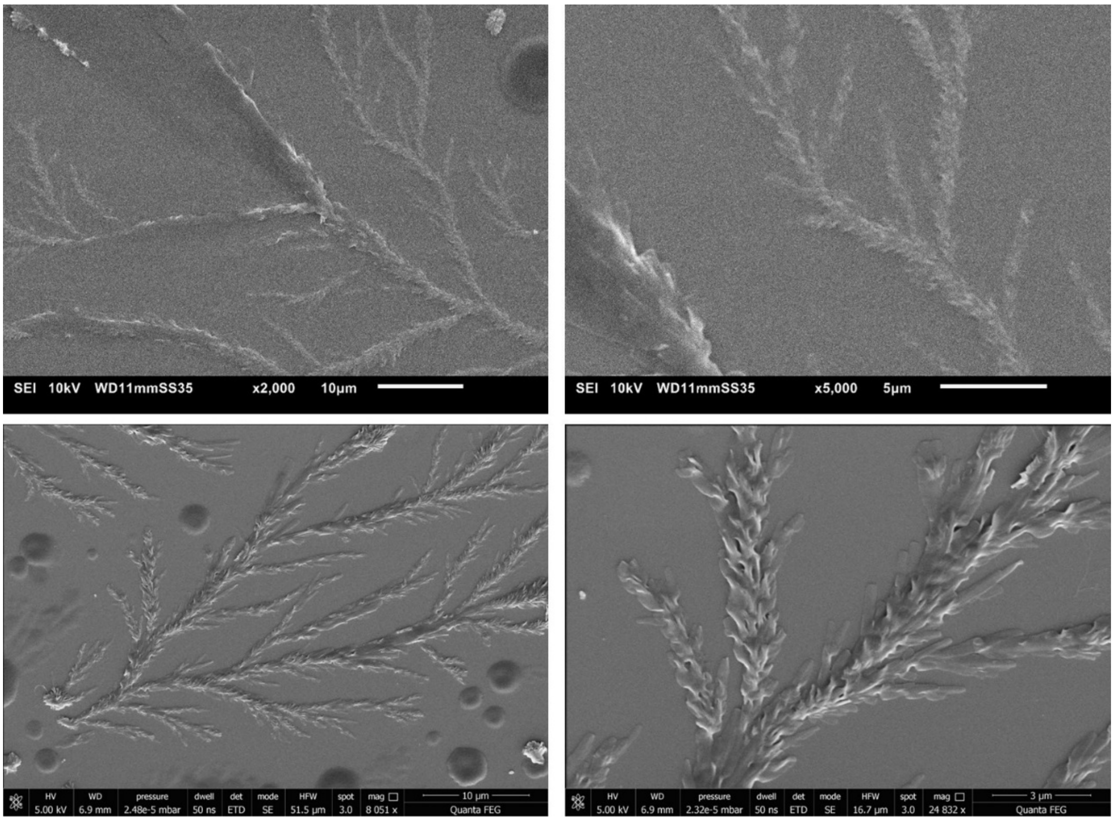

Fig. S1. Additional SEM images of the nanostructures formed by (*P*)-1 via drop casting its TCB solution on silicon surface at ambient condition. Concentration: 5×10^{-4} M.

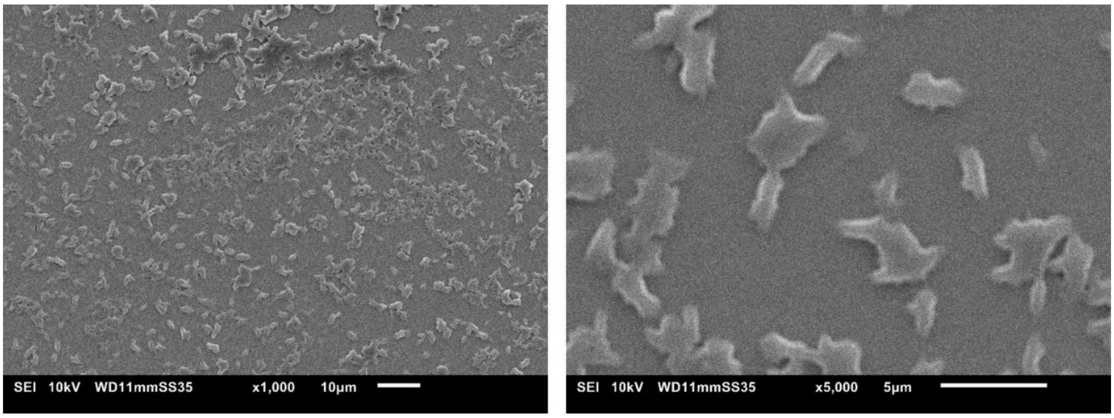

Fig. S2. Additional SEM images of the nanostructures formed by (*rac*)-1 via drop casting its TCB solution on silicon surface at ambient condition. Concentration: 5×10^{-4} M.

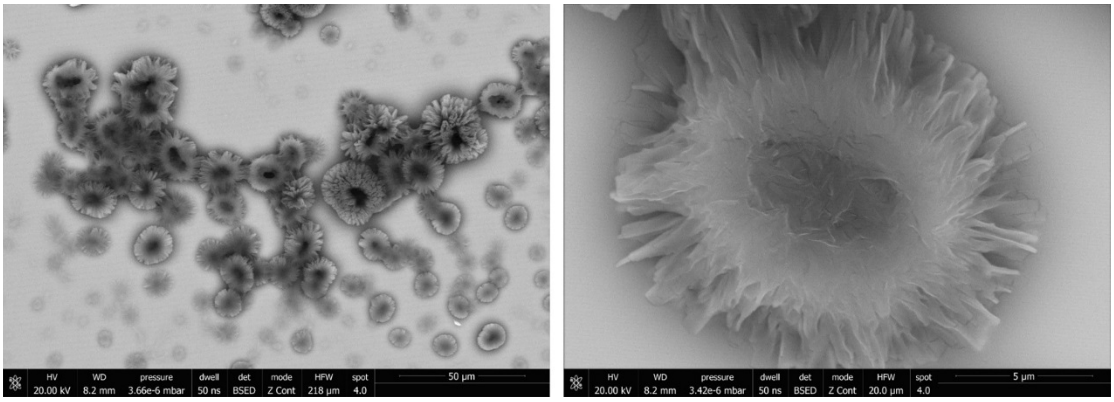

Fig. S3. SEM images of the nanostructures formed by (*P*)-1: (*M*)-1 = 3:1 via drop casting its TCB solution on silicon surface at ambient condition. Concentration: 5 × 10^{-4} M.

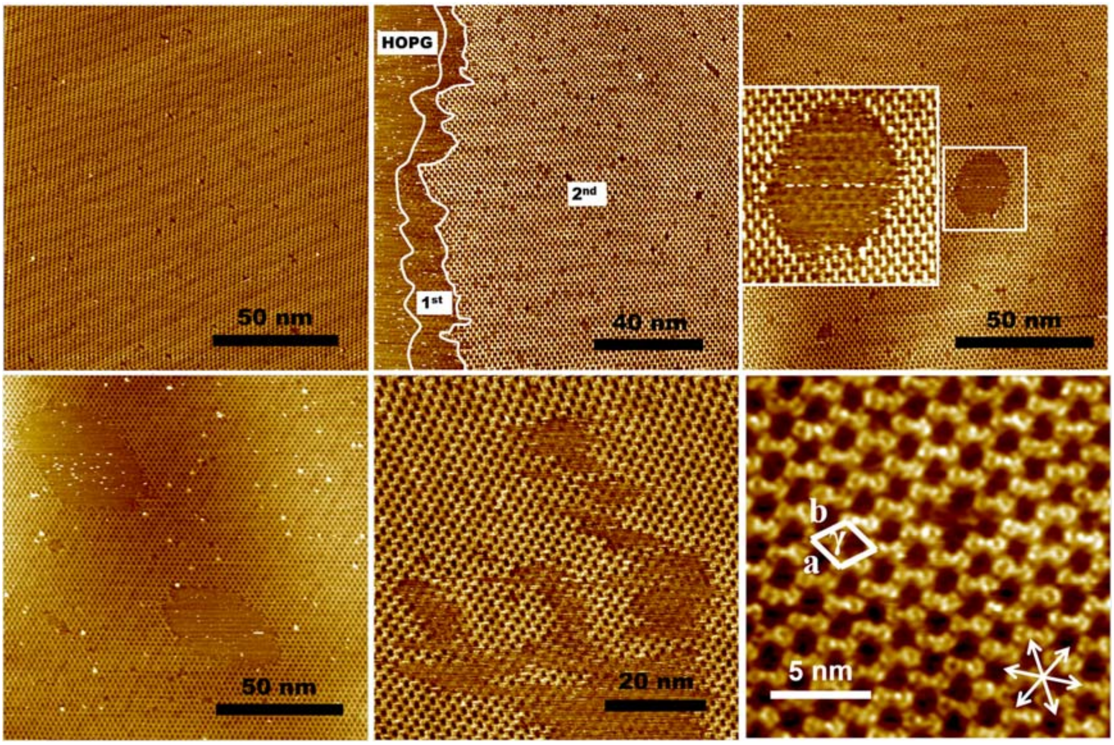

Fig. S4. Supplementary STM images of the surface pattern formed by (*rac*)-1 at the TCB/HOPG interface. Concentration: 5 × 10^{-4} M.

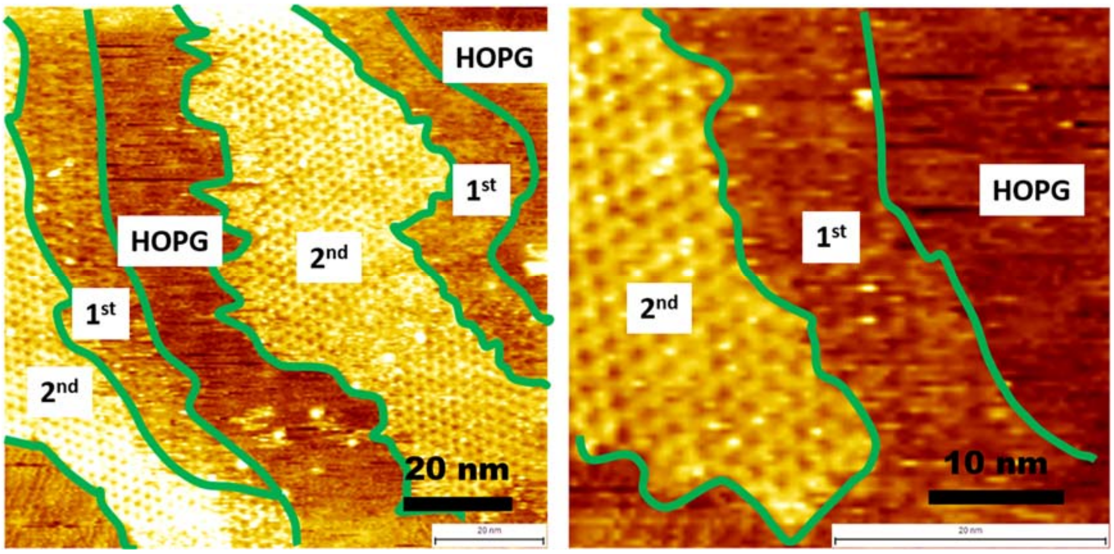

Fig. S5. STM images of the self-assembled networks of (*rac*)-1 at the phenyloctane/HOPG interface. Bilayers (2^{nd}), monolayers (1^{st}), and uncovered or mobile phases (HOPG) are indicated. I_{set} = 150 pA, V_{bias} = -1000 mV.

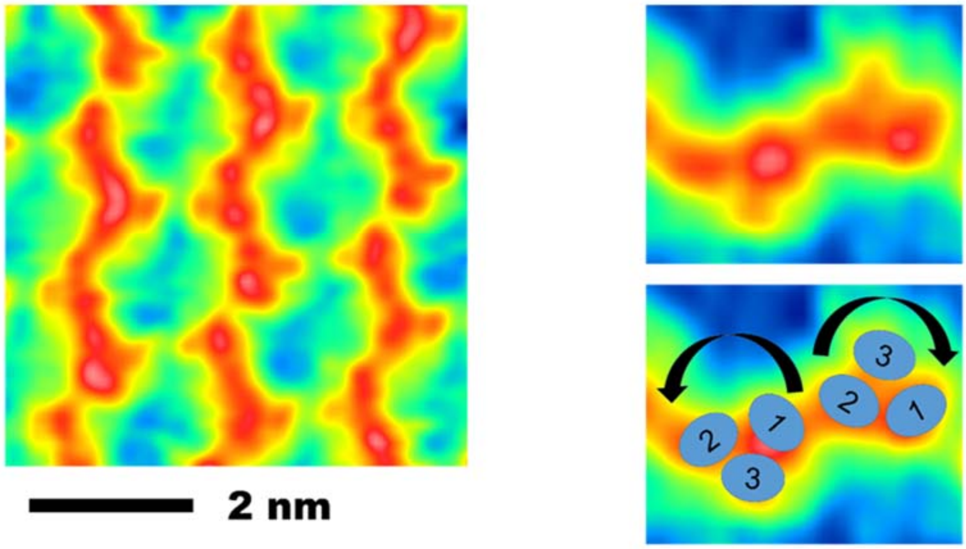

(*rac*)-1 on HOPG

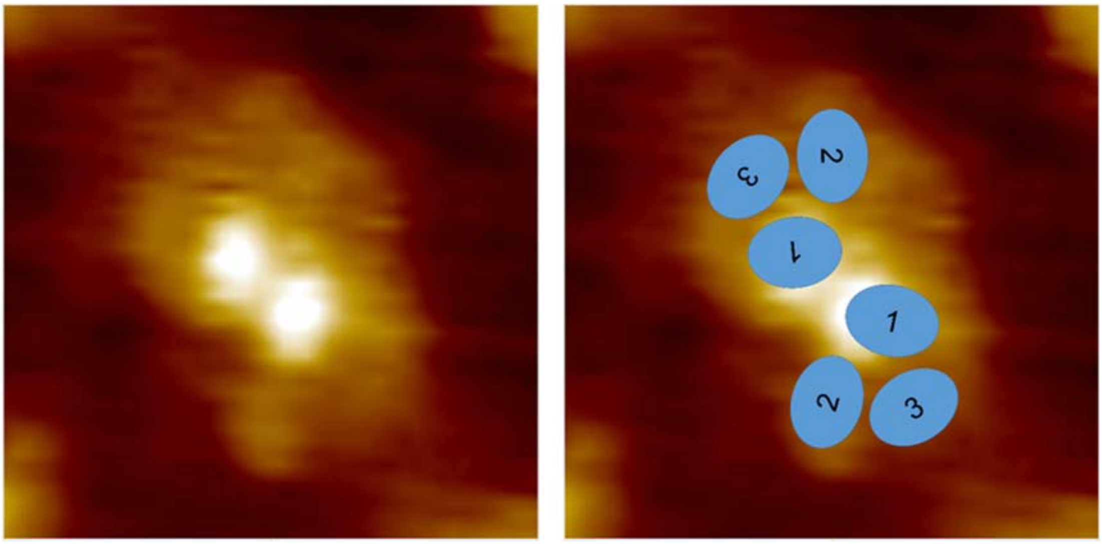

(*P*)-1 on Au(111)

Fig. S6. The absolute chirality of helicenes in a racemic network is assigned on the basis of a comparison of the contrast feature of (*rac*)-1 on HOPG and enantiopure (*P*)-1 on Au(111).

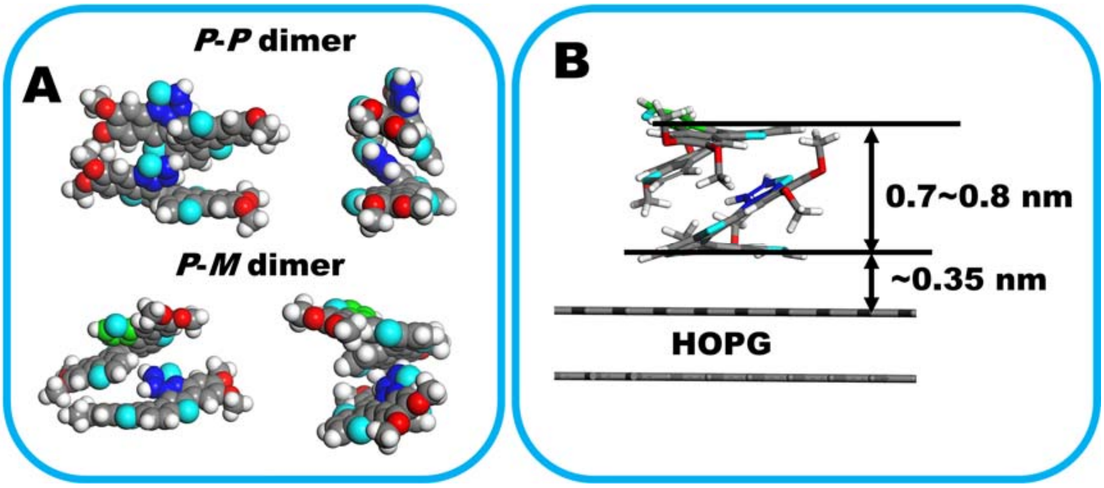

Fig. S7. (A) DFT simulation of *P-P* and *P-M* dimerization along the helix axis direction. Method: PBE1PBE/6-31G*. Due to the lack of support in the vicinity, the height of heterochiral dimer falls into the range of 0.4~1 nm. (B) Ideally, the opposite parallel oriented stacking of *P-M* dimer should amount to 0.7-0.8 nm in height. Taking account of the spacing between a bilayer and substrate (~0.35 nm), 1 nm should be ascribed to the height of a bilayer stacking of racemic helicene network.

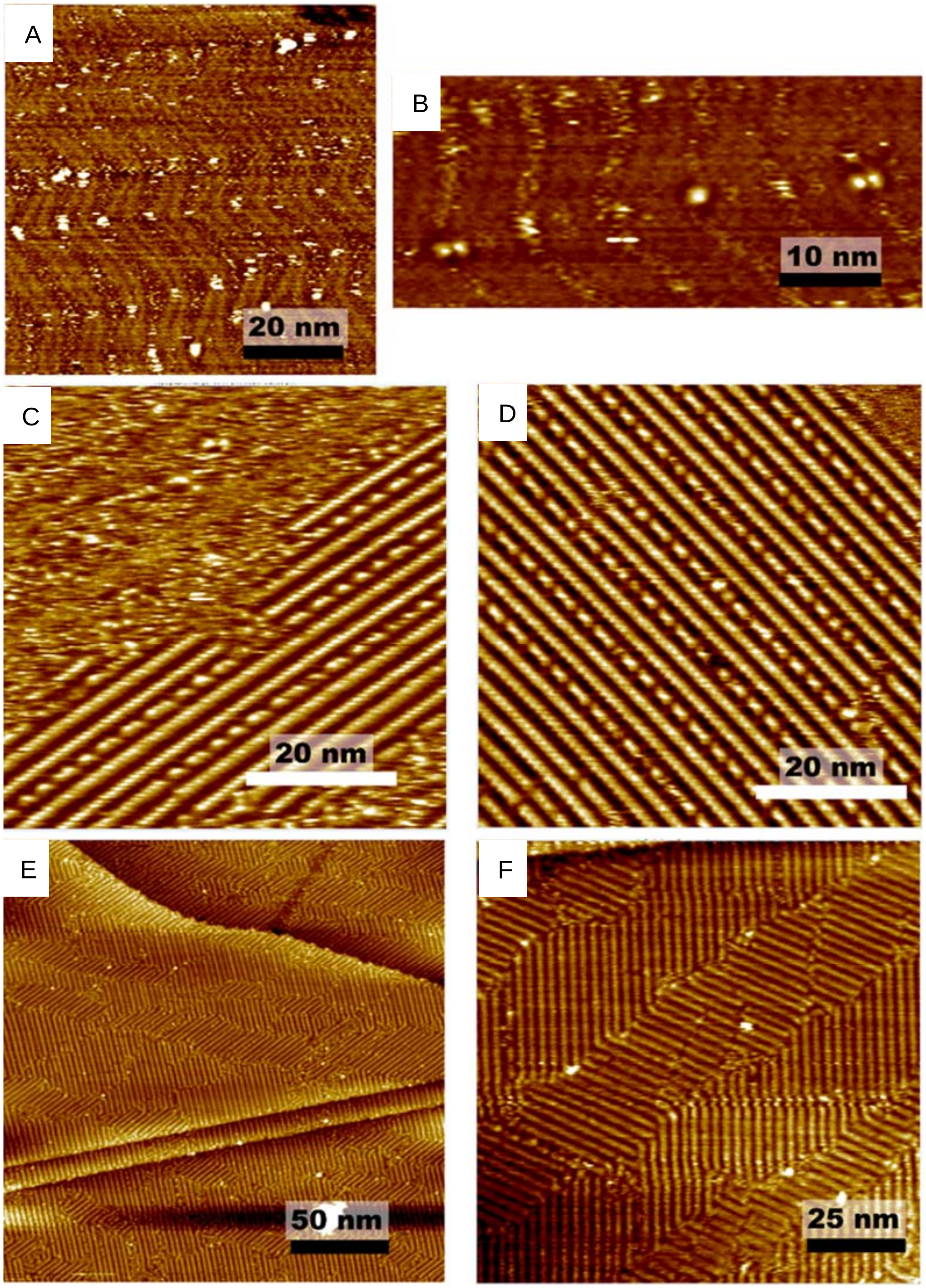

Fig. S8. Supplementary STM images showing the concentration-driven structural transition of (*P*)-1 on Au(111) surface. (A, B) At the concentration of 2 × 10^{-6} M in TCB, most clusters appear with fuzzy feature at the elbow sites of surface construction, as a result of the high mobility of small aggregate on surface, but some can be clearly identified. (C, D) Helicene rows separated by dimers and trimers, observed at the concentration of 5 × 10^{-6} M and 1 × 10^{-5} M. (E, F) Alignment of helicenes along the surface reconstruction, observed at the concentration of 5 × 10^{-5} M.

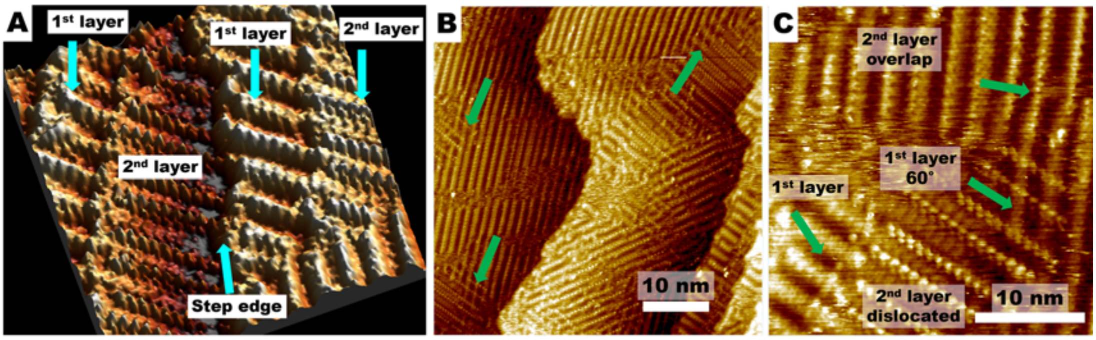

Fig. S9. Supplementary STM images showing the bilayer structure of (*P*)-1 on Au(111) surface. (A) 3D visualization of a bilayer stacking. (B, C) large and small scale STM images showing the crossing and the overlap of helicenes rows.

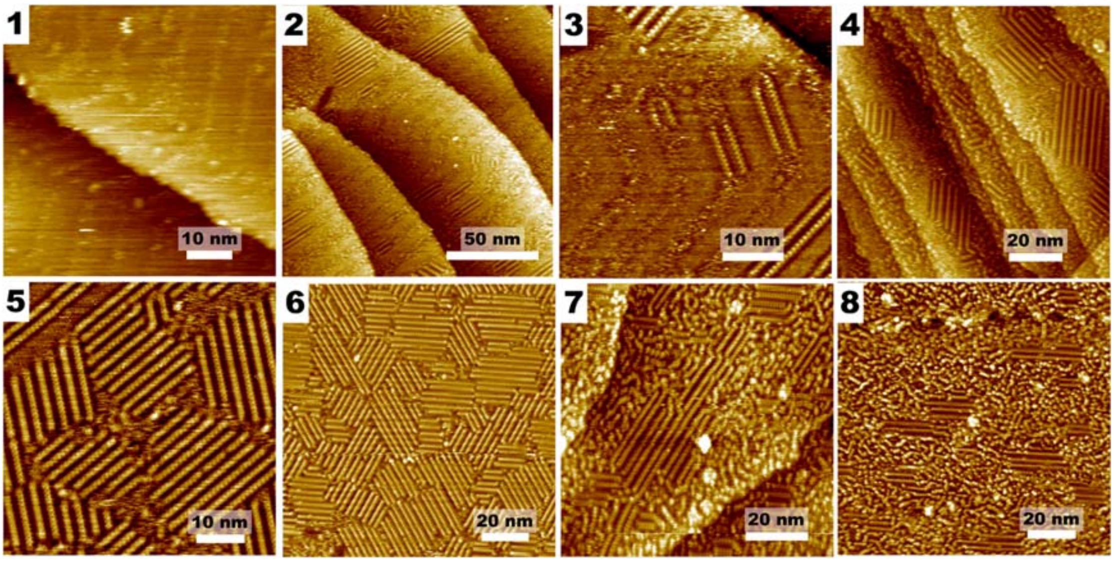

Fig. S10. Supplementary STM images showing the concentration-driven structural transition of (*rac*)-1 on Au(111) surface: (1) clusters at the elbow sites (2 × 10^{-6} M); (2, 3) Helicene rows, always even-numbered, grow along the ridge of surface reconstruction at sub-monolayer coverage (2 × 10^{-6} M and 5 × 10^{-6} M); (4) Small clusters appear along with helicene strands at sub-monolayer coverage (5 × 10^{-6} M). (5, 6) The coverage of linear structure becomes higher with the increasing of concentrations (5 × 10^{-6} M and 1 × 10^{-5} M). Note that the rows are aligned along three different orientations. (7, 8) Small clusters reappear when the surface reaches full coverage (2 × 10^{-5} M and 5 × 10^{-5} M).

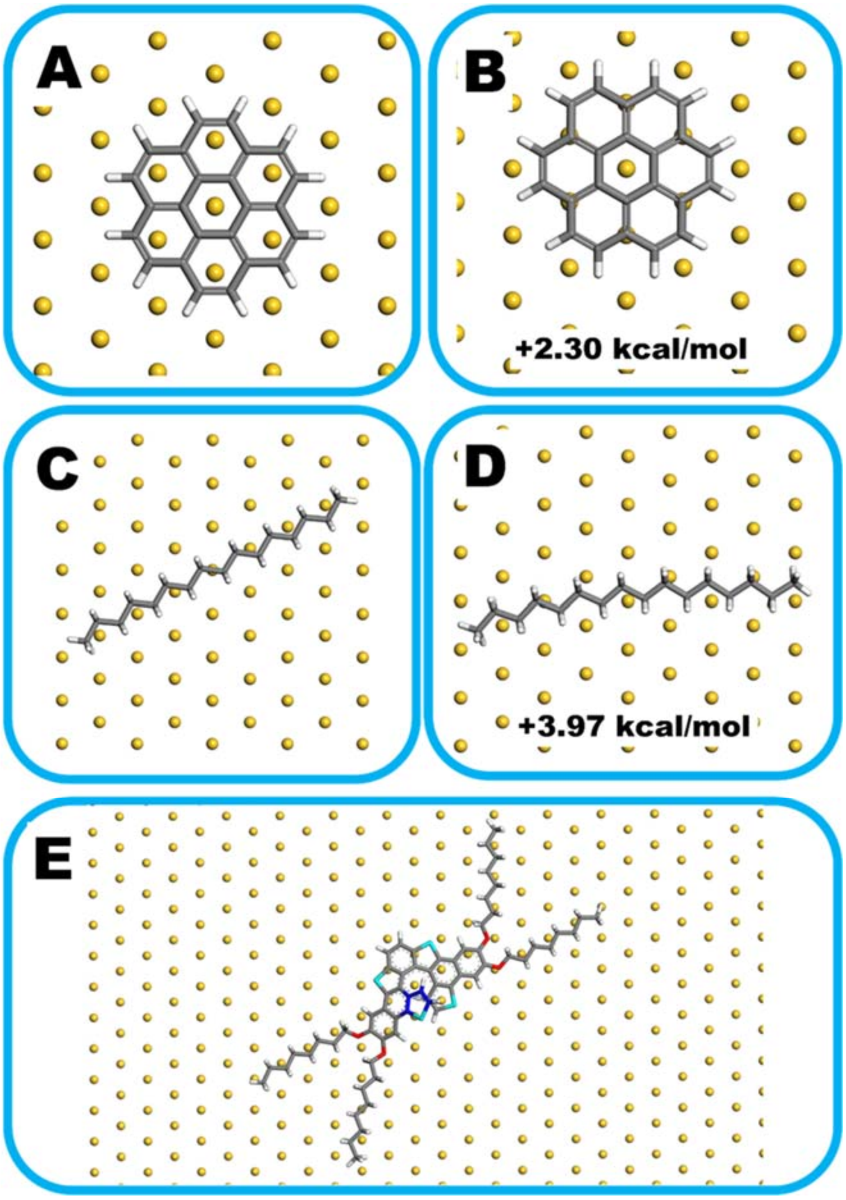

Fig. S11. Calculated models of (A, B) coronene and (C, D) $C_{16}H_{34}$ on Au(111) surface. In both cases, the absorbate was initially oriented along one of the symmetry axes of underlying substrate and optimized with Materials Studio, using the Forcite module with COMPASS force field. All simulations were performed under periodic boundary conditions. The substrates was frozen during the simulations, and a cutoff of 1.85 nm was applied for the van der Waals interactions. As we can see, COMPASS force field provides satisfied simulation on the commensurate packing arrangements of (A) coronene and (C) $C_{16}H_{34}$ on Au(111). (E) Therefore, the configuration of helicene was adjusted and optimized using the same protocol. Gray: C; white, H; red: O; light blue: S; yellow: Au; Blue: C atoms of the protruded thiophene unit of (*P*)-1.

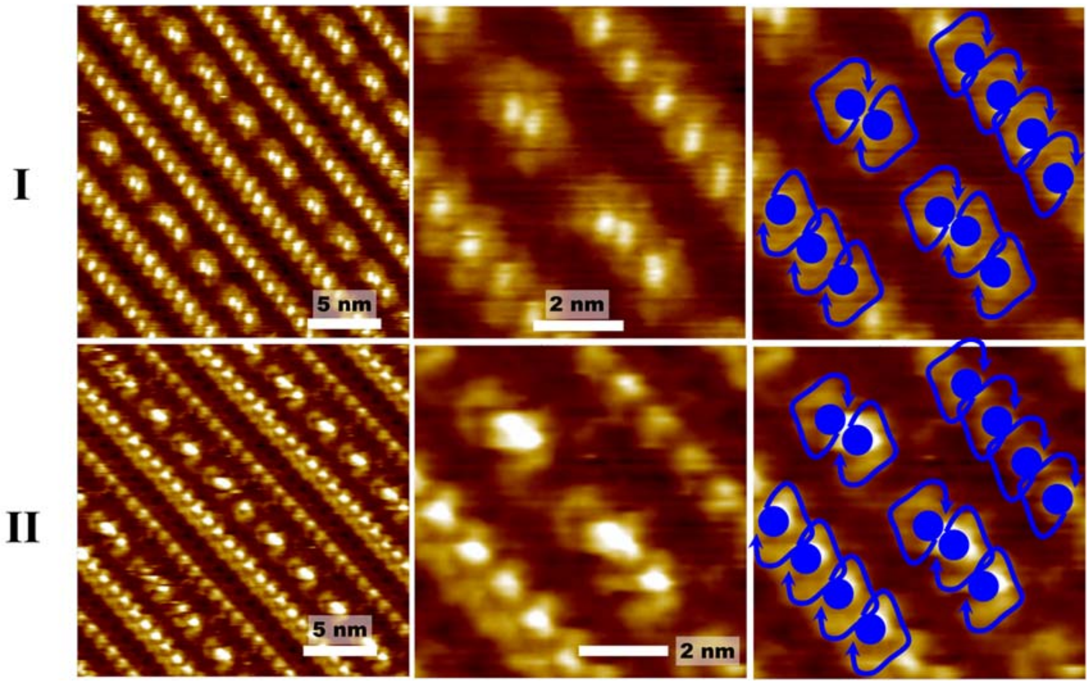

Fig. S12. Two different types of contrast of enantiopure (*P*)-1 on surface.

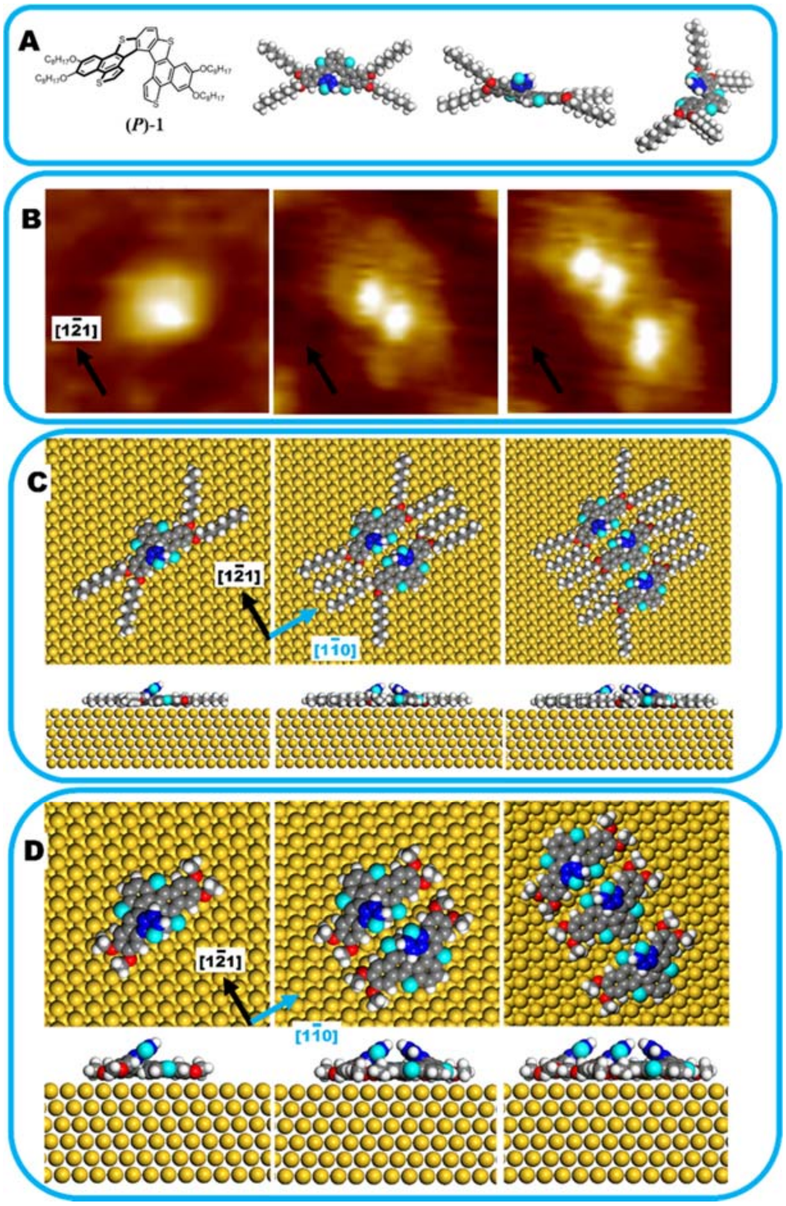

Fig. S13. (A) Optimized structure of (*P*)-1, using Gaussian software with B3LYP/6-31G(d,p) method. (B) Close-up STM images and (C, D) corresponding simulated models of surface-bound (*P*)-1 monomer, dimer and trimer. The initial arrangement of helicenes were conceived according to the STM observations. Simulation were performed with Materials Studio, using the Forcite module with COMPASS force field. All simulations were performed under periodic boundary conditions. The substrate, six-layer of gold surface, was frozen during the simulations, and a cutoff of 1.85 nm was applied for the van der Waals interactions. The substitution of (C) lateral alkyl chains with (D) methyl groups, however, does not bring visible changes the arrangement of helicenes, suggesting that the intermolecular interaction between aromatic moieties is decisive in determining the surface organization.

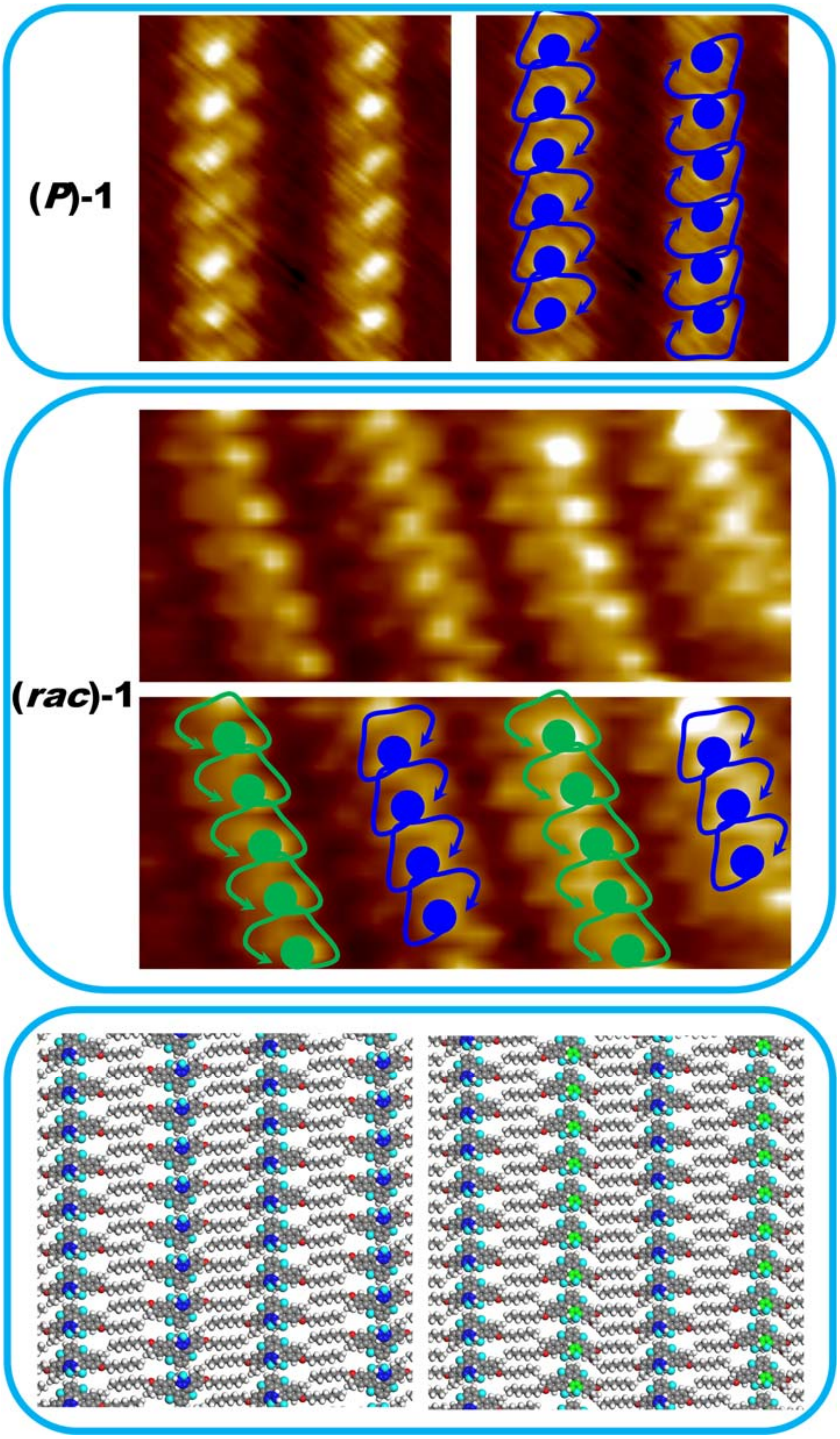

Fig. S14. High-resolution STM images and tentative structural models of homochiral and racemic linear networks of helicenes. (*P*)-1 and (*M*)-1 are differentiated with blue and green colour. Only two of the four lateral alkyl chains are displayed, as there is no enough space to accommodate all of them.

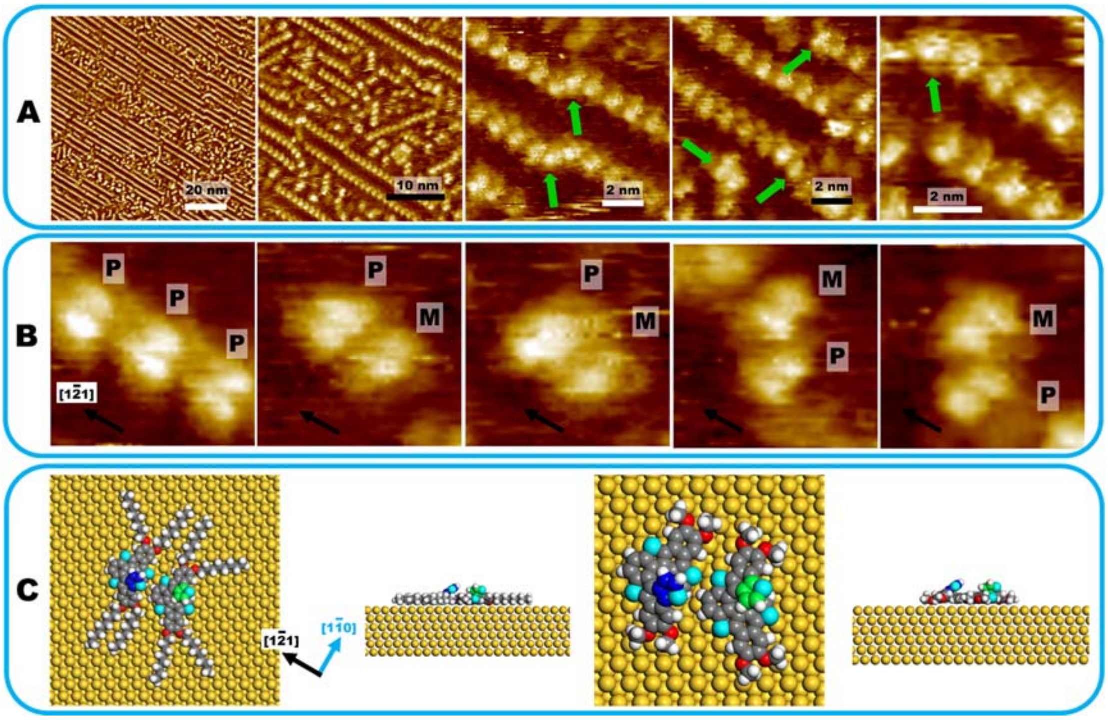

Fig. S15. (A) STM images of the self-assembled networks of (*P*)-1: (*M*)-1 = 95:5 at the TCB/Au(111) interface at the concentration of 5×10^{-4} M. Green arrows outline the helicenes with different orientation as compared to the majority helicene rows. (B) Close-up STM images of homochiral helicene row in comparison with the dimers of (*P*)-1 and (*M*)-1. Size: 3 nm × 3 nm. (C) Simulated structure model for a *P*-*M* dimer, using the same method described in the caption of Fig. S13.

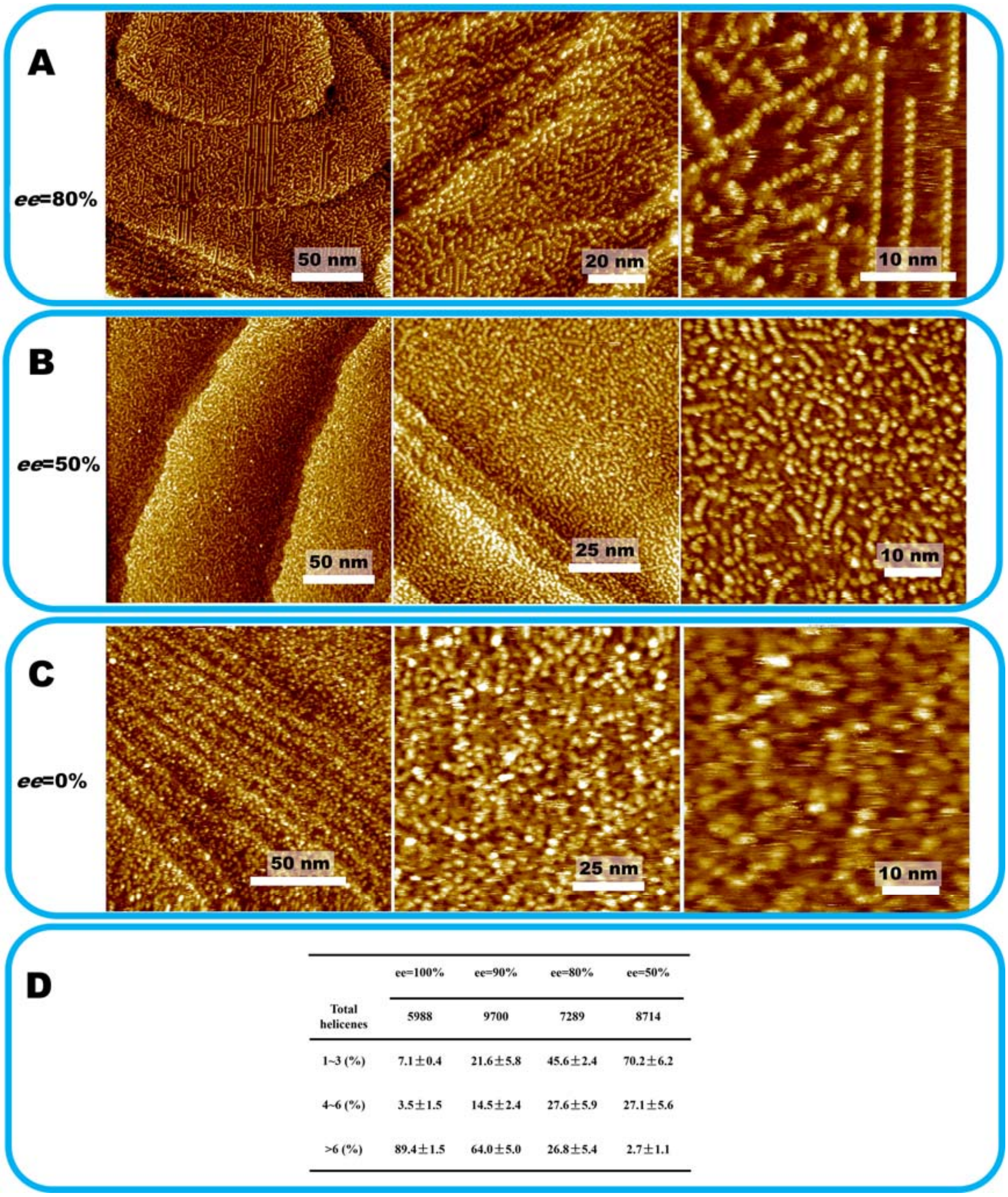

	ee=100%	ee=90%	ee=80%	ee=50%
Total helicenes	5988	9700	7289	8714
1~3 (%)	7.1±0.4	21.6±5.8	45.6±2.4	70.2±6.2
4~6 (%)	3.5±1.5	14.5±2.4	27.6±5.9	27.1±5.6
>6 (%)	89.4±1.5	64.0±5.0	26.8±5.4	2.7±1.1

Fig. S16. (A, B, C) STM images of the self-assembled networks of the mixtures of (*P*)-1and (*M*)-1 at the TCB/Au(111) interface, at a total concentration of 5×10^{-4} M. *ee* = ([*P*]−[*M*])/([*P*]+[*M*])×100%. (D) Statistics of the surface coverage of aggregates with different lengths (number of molecules in each column) as a function of *ee* values.

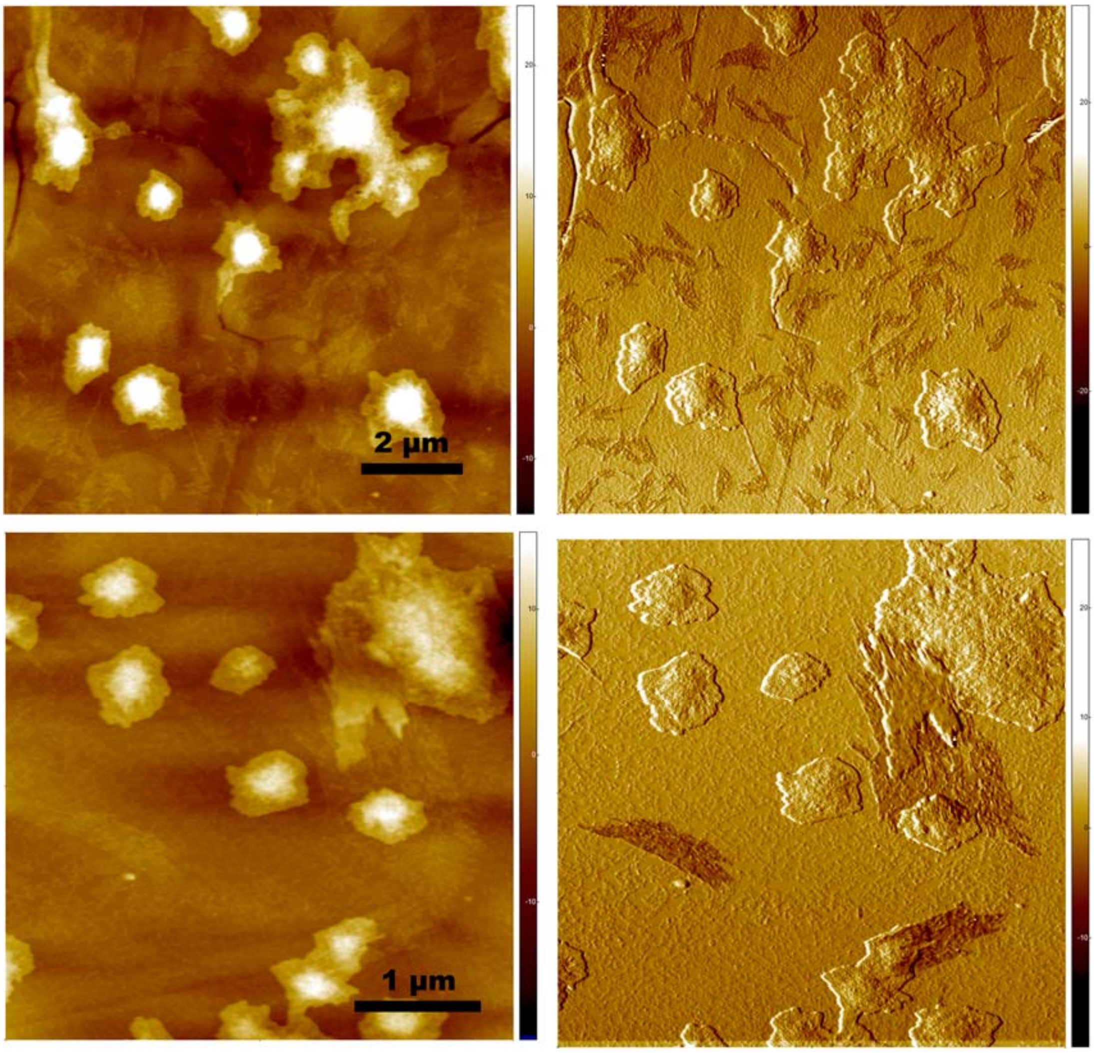

Fig. S17. AFM images of the structures of (*P*)-1 via drop casting its TCB solution on Au(111).

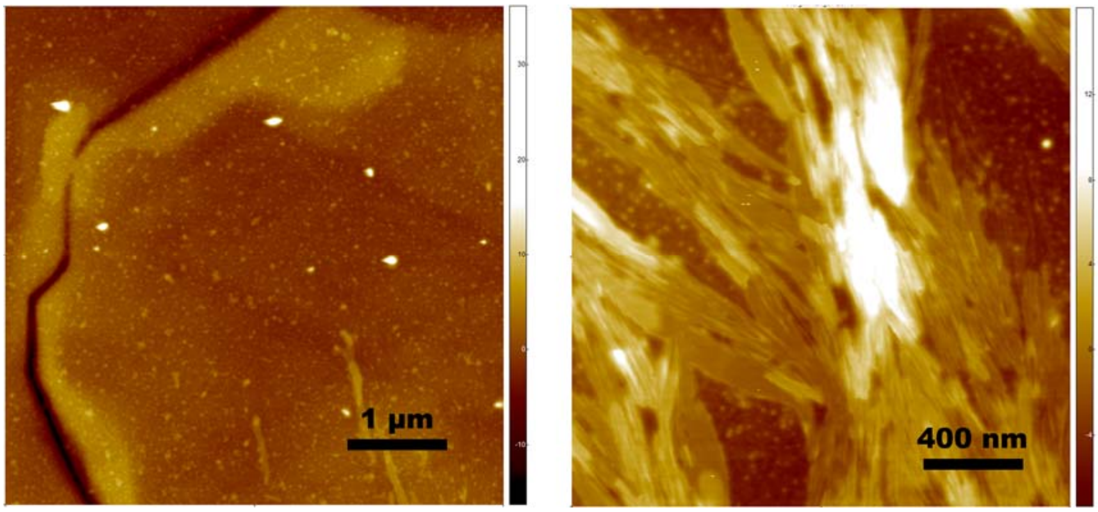

Fig. S18. AFM images of the structures of (*rac*)-1 via drop casting its TCB solution (5×10^{-4} M) on Au(111).